Microseismicity of the Béarn range: reactivation of inversion and collision structures at the northern edge of the Iberian plate

Thierry Dumont, Anne Replumaz, Stéphane Rouméjon, Anne Briais, Alexis Rigo, Jean-Pierre Bouillin

Microseismicity of the Béarn range: reactivation of inversion and collision structures at the northern edge of the Iberian plate

Thierry Dumont [a,*], Anne Replumaz [a], Stéphane Rouméjon [b], Anne Briais [c], Alexis Rigo [d] and Jean-Pierre Bouillin [a]

[a] Université de Grenoble I Joseph Fourier, CNRS, laboratoire ISTerre
BP 53, 38041 Grenoble Cedex, France, thierry.dumont@ujf-grenoble.fr
Tel.: 33 4 76 63 59 04 Fax: 33 4 76 51 40 58
* corresponding author

[b] Institut de physique du globe de Paris, 1 rue Jussieu - 75238 Paris cedex 05, France

[c] GET, CNRS/UPS/IRD, Observatoire Midi-Pyrénées, 14 ave. E. Belin - 31400 Toulouse, France

[d] Laboratoire de Géologie, ENS, CNRS, PSL Research University, 24 rue Lhomond, 75231 Paris Cedex 05, France

Key words

Microseimicity, deformation history, structural inversion, extensional reactivation, Western Pyrenees, Iberian plate margin

Abstract

The Béarn range, located to the north of the Axial Zone in the Western Pyrenees, is affected by numerous small magnitude seismic events. These events overlap an area characterised by specific geological structures which are interpreted to have resulted from multistage extensional and compressional deformation. An analysis of surface geology draped over DEM, together with field investigations, allow identification of two main shortening episodes with differing direction of contraction: D1 represents the inversion of the North-Pyrenean basin, whose Mesozoic infill was detached from highly extended crust and transported southwards over the necking zone and the northern margin of the Iberian plate; D2 corresponds to the collision stage, and is characterised in the study area by backfolding and backthrusting deformation coeval with uplift in the axial part of the chain due to thickening of the Iberian plate. The microseismicity appears to concentrate along the basal part of the inverted basin units (D1) where this initially low-angle thrust has been tilted and steepened during collision (D2). We propose that local steepening of this ancient inversion structure, which should not be named "North Pyrenean fault", provided the suitable dip for extensional solicitation in association with the present uplift of the Axial Zone, whatever the driving mechanism of this uplift could be.

1. Introduction

Several techniques allow description of the deformation field in areas of active continental deformation. Some focus on short time scale deformations (≤ 100 yrs), such as measurements of surface displacement by GPS, or radar interferometry, or analysis of seismicity. Other techniques, which address longer time scales, focus on fault slip-rate, estimated from the paleoseismicity or the dating of paleo-river terraces or channel offsets (e.g. Chevalier et al., 2005, Lasserre et al., 1999; Replumaz et al., 2001). In areas undergoing rapid deformation, all these different techniques may be applied. Although they do not always provide a coherent picture, they can be used to interpret the geological framework and the landscape morphology. In orogens where the deformation rate is low, few of these techniques are efficient, and their results are often ambiguous. This is the case for the Pyrenees range, a 400 km-long range with an elevation frequently exceeding 2000m, which results from the relative motion of the Iberia and Eurasia plates. Models implying a range under either compression or extension, with rates lower than 0.5 mm/yr, are both compatible with the available geodetic data, according to geodetic measurements across Europe and North Africa (Nocquet and Calais, 2003) or to local continuous GPS stations (Asensio et al., 2012; Rigo et al., 2014). Surface rupture related to Holocene seismic activity has not been unambiguously documented by neotectonics studies so far. In the northern frontal zone, folding of young fluvial

Tectonics, 34, **DOI:10.1002/2014TC003816**

terraces with about 7m of uplift has been clearly observed near Arudy, but there is no evidence of faulting (Lacan et al., 2012). Near Lourdes the border of a fluvial valley parallel to the main structures can be interpreted either as a normal fault, but without any surface rupture observed (Alasset and Meghraoui, 2005), or as a river bank. In the highest part of the chain some geomorphic and subsurface geophysical studies have led to the interpretation of north-dipping normal faulting but, again, with no surface rupture (Lacan and Ortuño, 2012). The attempts to determine a regional stress field using inversion of P wave polarities have long failed (Nicolas et al. 1990; Delouis et al. 1993), even with temporary local networks (Gagnepain et al. 1980; Gagnepain-Beyneix et al. 1982; Rigo et al., 2005). Recently, using waveform inversion, Chevrot et al. (2011) have determined extensional focal mechanisms for all but one event (Mw>3) between 2001 and 2011, suggesting that the most probable current deformation regime of the range is extension.

Despite the low deformation rate, the seismic activity of the range is characterized by numerous small magnitude events, and several events of moderate magnitude ($4 \leq Ml < 6$). A seismic cluster persistent through time is observed between Bagnères-de-Bigorre and Oloron, as a 10 km-wide, 100 km-long, E-W trending stripe (Fig. 1). On cross-sections, the cluster appears as a vertical to north-dipping zone, which has previously been interpreted to be linked to the so-called North Pyrenean Fault, considered to be the vertical plate boundary between Iberia and Eurasia (e.g. Gagnepain-Beyneix et al. 1982; Souriau and Pauchet, 1998), prior to the collection of subsequent event location data which has revealed that the seismic cluster probably does not coincide with the inferred fault trace (Souriau et al. 2001; Dubos, 2003; Rigo et al. 2005). Thus, despite the deep structure of the range having been constrained by 2 seismic profiles, ECORS-Arzacq to the west of the study area and ECORS-Pyrenees in the central part of the chain, the structures responsible for this seismic cluster and its geometry at depth are not yet identified accurately. In this paper, we reassess the surface geology and cross-sections to propose a new interpretation to explain these seismic events in the context of the regional deformation regime. Cross-sections are utilised to illustrate the lateral variation in shortening, which is interpreted to be relatively high east of Lourdes and lower to the west of Oloron. We demonstrate that the structure changes geometrically along the length of the range, but that there does appear to be regional consistency of structural style at depth based on our serial cross-sections, which integrate previously published information (e.g. Dubos-Sallee et al., 2007; Lacan, 2008; Lacan et al., 2012).

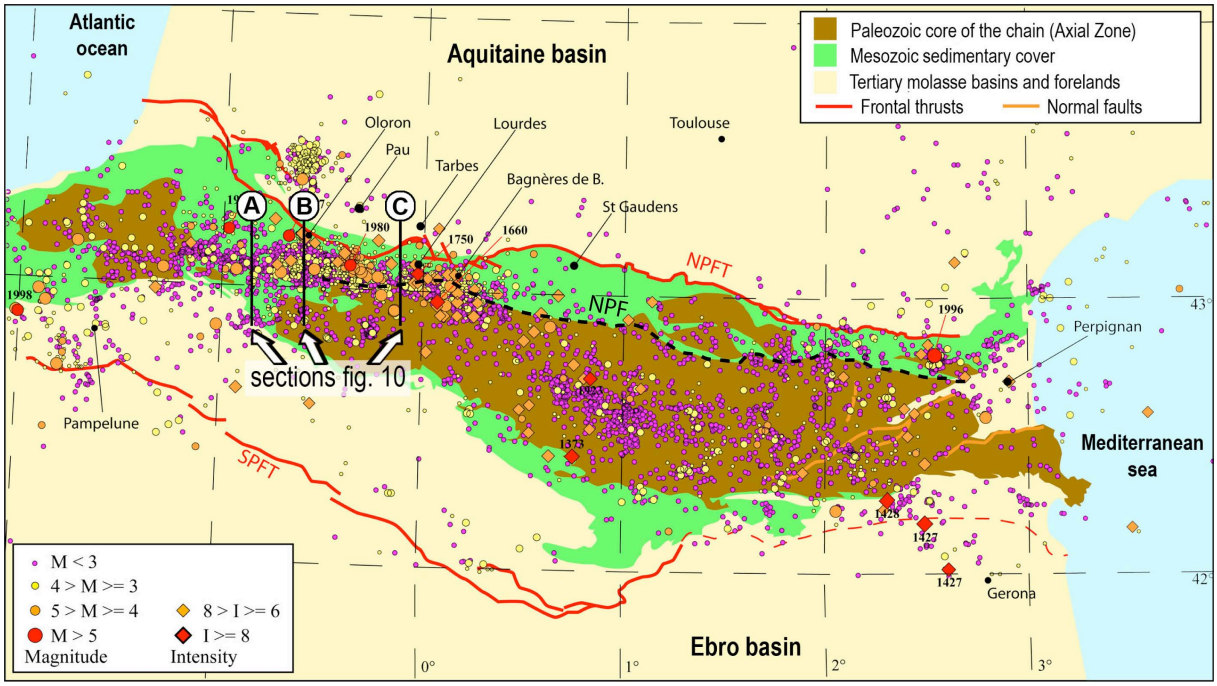

Figure 1: *Seismotectonic map of the Pyrenean range showing the location of the seismicity within the upper crustal Axial Zone and folded Mesozoic sediments. Catalogue from OMP-IGC (Observatoire Midi Pyrénées-Institut Geològic de Catalunya); for more detail see Souriau et al., 2001; Chevrot et al., 2011), data ranging from 1997 to 2011. A cluster of micro and moderate magnitude events is observed on the northern side of the range, between Oloron and Bagnères-de-Bigorre. North of this cluster, the frontal thrust is close to the range axis. NPFT: North Pyrenean Frontal Thrust. SPFT: South Pyrenean Frontal Thrust. The black dashed line corresponds to the historically assumed trace of the North Pyrenean Fault (i.e. Choukroune, 1992). The cross sections of Fig. 10 are located.*

2. Geological and Geophysical settings

2.1 From rifting to inversion

The relative motion of the Iberia and Eurasia plates since the Middle Cretaceous has remained a matter of debate over the past 30 years, and no consensus has been reached yet either about the initial position of Iberia or on the exact timing of events (Olivet, 1996; Sibuet et al., 2004; Jammes et al., 2009). Extension, in addition to left-lateral motion, occurred before and during the opening of the Bay of Biscay between the 2 blocks. Following the deposition of the shallow-water Jurassic sequences which record some distant effects of the Tethyan margin subsidence (Puigdefabregas and Souquet, 1986 ; James et al., 1996), a widespread uplift and emergence of the southern rift flank occurred between Late Jurassic and Early Aptian in the areas now forming the core of the chain. The resulting sedimentary gap, marked by continental alteration (bauxites), was initiated as early as the Late Jurassic (Combes et al., 1998). The underlying sedimentary wedges are increasingly truncated towards the southern rift shoulder presently represented by the Axial Zone, over which the whole syn-rift and part of the pre-rift sediments are missing (Fig. 2; Teixell, 1996). The syn-rift extension is also demonstrated by Aptian-Albian block tilting (Souquet et al., 1985; Ducasse et al., 1986a; Vélasque et al., 1989; Lenoble and Canérot, 1993) and halokinesis (Canérot, 1989; Bourrouilh et al., 1995; Biteau et al., 2006).

The major extensional phase resulted in crustal attenuation, possibly involving a N-dipping crustal-scale detachment (Velasque et al., 1989) along which the sedimentary cover could have slid (Johnson and Hall, 1989; Jammes et al., 2009; Lagabrielle et al., 2010; Masini, 2011). Extreme crustal thinning is required to explain the occurrence along the northern boundary of the Iberian plate of exhumed upper mantle and lower crustal rocks as early as Middle Cretaceous (Henry et al., 1998; Debroas et al., 2010; Lagabrielle et al., 2010), along with evidence for HT-LP metamorphism having affected the Mesozoic sedimentary cover at about the same time (Uppermost Albian to Turonian; Albarède and Michard-Vitrac, 1978; Montigny et al., 1986; Goldberg and Leyreloup, 1990; Azambre et al., 1991), and for coeval magmatic activity in the North Pyrenean basins (Montigny et al., 1986).

From Middle Albian to Early Cenomanian, the central part of the rift was filled by up to 4 km of deep water flysch-type deposits (Souquet et al., 1985). The distribution of the Albian basins has been explained as a response to transtensional deformation (Peybernès and Souquet, 1984; Puigdefabregas and Souquet, 1986; Debroas, 1990; Bourrouilh et al., 1995) in particular in the Basque-Cantabrian area (Aguirrezabala and Garcia-Mondéjar, 1992; Soto et al., 2011).

The resulting structure of the basin can still be recognized after its inversion, and includes three main zones on the northern side of the orogen (Fig. 2): **Zone 1** corresponds to the Mesozoic cover of the so-called North-Pyrenean zone, derived from the central part of the rift; **Zone 2** consists of intermediate units whose series show abundant erosion/resedimentation features (Mendibelza and Igountze conglomerates; Boirie and Souquet, 1982), and which are derived from the rift flank; **Zone 3** is represented by the so-called Axial Zone, presently the most uplifted part of the range, and comes from the northern edge of the Iberian plate, formerly in a rift shoulder setting (Fig. 2). These different zones are characterized by specific tectono-stratigraphic signatures, with an overall southward pinching-out of the Jurassic-Cretaceous formations (Fortane et al., 1986). A sedimentary gap, corresponding to both erosion and continental non-deposition, is present across the three zones with a southerly increase in duration of the gap (Canérot et al., 1978). The duration of the gap depends on both the northward propagation of the rift shoulder uplift from Kimmeridgian to Neocomian (Combes et al., 1998) and the south-directed onlap of the post-rift sediments towards the Iberian margin.

The early stages of compression are characterised by structural inversion of the Cretaceous rifts (Beaumont et al., 2000) possibly involving reverse reactivation of a north-dipping low-angle detachment (Velasque et al., 1989) with south-directed shortcuts along the rift shoulder (Ducasse et al., 1986a and b; Teixell, 1996). Structural inversion is detected within the Mauléon basin using Anisotropy of Magnetic Susceptibility analysis (Oliva-Urcia et al., 2010), providing evidence for NS to NE-SW shortening consistent with the NNE-SSW direction of compression (Bourrouilh et al., 1995) and with S-SW transport directions of thrust-sheets (Lakhoura thrust: Velasque et al., 1989). This inversion is related to the northward subduction of the Iberian crust in the western Pyrenean and Cantabrian domains (Ducasse et al., 1986b; Ferrer et al., 2008) and a part of the margin edge is suspected to have been underthrust beneath the inverted basin (Velasque and Ducasse, 1986). Within the Pyrenean chain, the amount of Alpine shortening increases from west to east, as expected from geodynamic constraints due to anti-clockwise rotation of Iberia (Olivet, 1996; Sibuet et al., 2004; Jammes et al., 2009). This is corroborated by the eastward increase in occurrence of mylonitic shear zones (Soula et al., 1986) and in total minimum shortening across the chain (Séguret and Daignières, 1986), whose estimates are based on crustal-scale cross-section balancing which suggest a range from 80 km in the western part (Teixell, 1998) to 125 or 147 km in the eastern part (Muñoz, 1992; Verges et al., 1995).

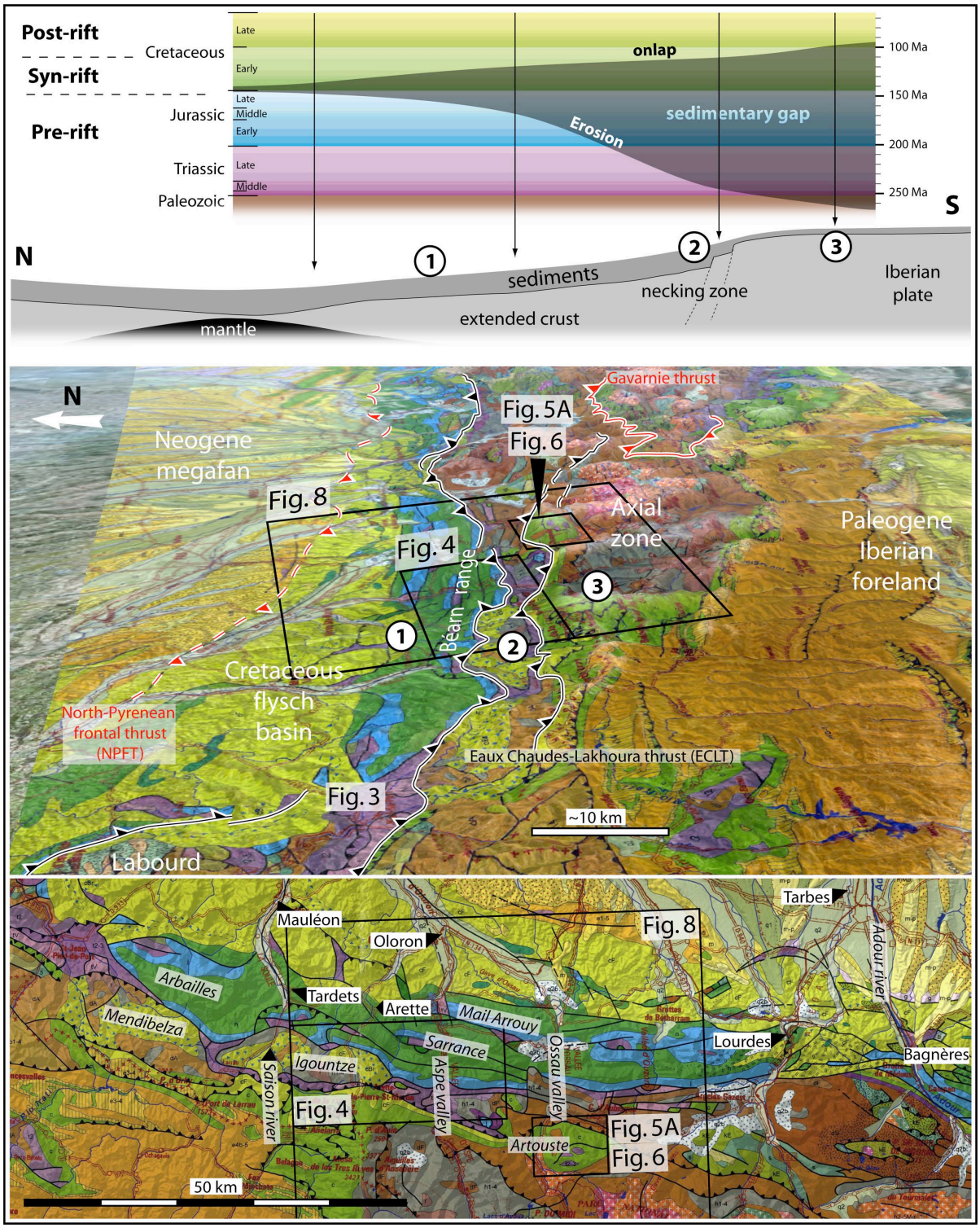

Figure 2: *Lower part: map view of the study area (extract from the 1/400000è geological map from BRGM/IGME) with the main locality names.*

Middle part: east-directed perspective view of the western part of the Pyrenees, showing the 1/400000è geological map from BRGM/IGME draped over the GoogleEarth DEM, with location of the three zones (see text §2): 1- North Pyrenean zone (Bearn range); 2- Intermediate zone; 3- Axial Zone. Also shown location of Figures 3, 4, 5A, 6 and 8.

Upper part: schematically restored profile from the Iberian plate to the north-Pyrenean basin during Cretaceous, showing the paleogeographic origin of the three zones (1-3). The Mesozoic series across it were characterized by a southward increasing sedimentary gap due to the combined effects of rift shoulder uplift (erosion) and post-rift continentward onlap (upper diagram).

2.2. Distribution of the seismicity within a very low convergent range

The permanent seismological network in the Pyrenees facilitates the production of maps with a good quality event detection threshold and location (Souriau and Pauchet, 1998). In 1997, the network quality increased (Souriau et al., 2001), with an event detection threshold as low as $M \geq 1$. The event location precision reaches ±1.5 km horizontally and ±3 km vertically.

The seismic activity of the range revealed by this OMP-IGC (Observatoire Midi Pyrénées-Institut Geològic de Catalunya) catalogue is characterized by numerous events of small magnitude, and several events of moderate magnitude ($4 \leq Ml < 6$) (Souriau et al., 2001; Chevrot et al., 2011). It is difficult to connect this activity with outcropping active structures, because significant activity is neither observed beneath the North Pyrenean Frontal Thrust (NPFT, figs. 1 and 2), nor below the Axial Zone, where several thrust units are known. A seismic cluster is observed between Bagnères-de-Bigorre and Oloron (Fig. 1) more or less parallel to the so-called "NPF", but not coinciding exactly with the inferred fault trace (Souriau et al. 2001; Dubos, 2003; Rigo et al. 2005). West of Lourdes, the cluster is located beneath the Mesozoic sedimentary cover. It intersects the "NPF" south of the city, and continues within the Palaeozoic Axial Zone east of it (Fig. 1). Lacan (2008) and Lacan and Ortuño (2012) have reported some post-orogenic normal reactivation of thrust faults in the highest part of the range, on the southern border of the seismic cluster. Except for that, the cluster spreads beneath the outcropping structures, and does not seem to be related to any particular fault. However, on cross-sections, the cluster appears as a vertical to north-dipping stripe (e.g. Gagnepain-Beynex et al., 1982; Souriau and Pauchet, 1998). In the following discussion, our serial cross-sections show that this cluster can match an important structure clearly connected with the surface geology.

2.3. Structure of the range

The Pyrenean chain has been frequently described as a doubly-vergent orogen developed at the northern edge of the Iberian plate (Choukroune, 1976; Séguret and Daignières, 1986; Muñoz, 1992; Daignières and ECORS team, 1994). The range is asymmetric with respect to the Axial Zone, with a wide southern flank and a narrow, steeper northern flank. On the southern side, several northward dipping thrusts which are rooted on low-angle decollement layers control the southerly propagation of the range with linked thrust network development far into the foreland (Fig. 1; Muñoz, 1992, 2002; Teixell, 1998). The amount of shortening increases from west to east, as well as the offset along the frontal thrust (Lacan, 2008). Thus the geological structure of the Pyrenean chain before the onset of compressional deformation can be restored more easily in the western part, whereas it has been strongly overprinted in the central and eastern parts.

The northern flank of the range is much narrower. The distance between the northern frontal thrust (NPFT) and the range axis varies from ≈60 km to the west, between the Atlantic coast and Oloron, to ≈20 km between Oloron and Bagnères-de-Bigorre, and to ≈40 km between Bagnères-de-Bigorre and Perpignan. The estimated offset along the northern frontal thrust also varies for each segment but in a different way (Lacan, 2008): 20 km from the west coast to Oloron, 5 km from Oloron to Bagnères-de-Bigorre, 30 km from Bagnères-de-Bigorre to Perpignan. In the eastern and western zones, two seismic profiles constrain the structure of the northern part of the range. To the west, the ECORS-Arzarq profile shows a low-angle, south-dipping frontal thrust (Grandjean, 1994; Daignières and ECORS team, 1994). The range spreads far northwards in the retro-foreland and grows horizontally, resulting in less asymmetry in this portion of the range. To the east, the ECORS-Pyrenees profile shows a steeper, south-dipping frontal thrust (Roure et al., 1989). The range is narrower and grows more vertically. Crustal indentation has been put forward to reconcile the doubly-vergent superficial geometry with north-dipping subduction of the lower Iberian crust (Teixell, 1998). Some authors emphasized a northward displacement of the extensional basin system considering the apparent predominance of north-verging thrusts and folds in the present-day structure (Séguret and Daignières, 1986; Baby et al., 1988; Lacombe and Mouthereau, 1999; Lacroix et al., 2012). Alternatively, other authors consider south-directed thrusting as the dominant inversion process, with a southward propagation of the thrusting sequence progressively shortcutting the northern edge of the Iberian plate (Ducasse et al., 1986b; Velasque et al., 1989; Teixell, 1996), which appears more consistent with a N-dipping continental subduction as generally proposed (Daignières and ECORS Team, 1994; Pedreira et al., 2007; Ferrer et al., 2008; Jammes et al., 2009).

The structure of the Béarn range is not constrained by any deep seismic profile. We examined the surface geology to infer its structure, and especially to explain the short distance between the frontal thrust and the range axis, and the minor offset observed along the frontal thrust. One of the specific implications of our preferred scenario is to involve two opposite verging events occurring successively, which correspond to north-directed continental subduction and to collision-related backfolding, respectively.

3. The Béarn range: evidence for two-stage Alpine deformation history

Shortening remains moderate in the Béarn range (zone 1, Fig. 2). The large-scale deformation of the sedimentary cover and upper basement units is examined, and the structure at depth of the main boundary

surfaces is interpreted using panoramic views, 3D geological information and field investigations. Our serial cross-sections show the consistency between the surface maps and interpreted deep structures, depict the lateral evolution of the structure along the Béarn range and make it possible to infer a plausible tectonic scenario for building the present orogen. Further on (section 4), a medium and small-scale field structural analysis of a key area is presented, in order to validate this scenario and the deformation history (section 5). Finally (section 6) we compare this interpreted deep structure with the distribution of the microseismicity (Fig. 1).

In the study area, the so-called North-Pyrenean zone corresponds to the Béarn massif (zone 1, Fig. 2), mostly made of Mesozoic cover outcrops derived from the Cretaceous basins; the Axial Zone is the most uplifted part of the range, corresponding to the Cretaceous rift shoulder at the northern edge of the Iberian plate (zone 3); in between is an intermediate structural unit derived from the slope between the rift shoulder and the basin, which shows abundant erosion/resedimentation features (zone 2). The stratigraphy in the North-Pyrenean zone thins southwards and is affected by a southward increasing Lower Cretaceous sedimentary gap, generated during the evolution of the rift shoulder (Fig. 2). The three zones are separated by thrust contacts which are discussed in the following section, and they are bounded from the retro-foreland domain to the north by the "North-Pyrenean Frontal Thrust" (NPFT, Figs. 1 and 2).

- The sedimentary gap is of moderate amplitude to the north (zone 1), as only Uppermost Jurassic and Lowermost Cretaceous strata are missing. The structure is characterised by steep northerly dips, due to northward-directed deformation and they form the northernmost important relief of the range. Closer from the southern boundary of the NPZ (southern part of zone 1), the sedimentary gap is of longer duration, ranging from Middle Jurassic to Middle Cretaceous (Lenoble and Canérot, 1993).

The panorama of Fig. 3 shows the tectonic contact between zones 1 and 2. Within zone 1 (Arbailles syncline, close to its southern boundary), the sedimentary gap ranges from Latest Jurassic to Early Cretaceous. Further south within zone 2, the intermediate units of the Mendibelza range display a major gap with missing strata ranging from Lower Triassic to Middle Cretaceous (Boirie and Souquet, 1982). The Lower Cretaceous carbonate series of the Arbailles syncline show overturned, northward-verging folds and are overthrust by the units of the Mendibelza range (Casteras, Paris et al., 1971). In the uppermost outcrops, the south-dipping faulted contact between the older Arbailles formations to the north (Aptian carbonates of zone 1, left part of the photo) and the younger Mendibelza formations to the south (Albian-Cenomanian flysch of zone 2, right part of the photo) gives the impression of a normal fault, but this is only because the thrust contact, initially dipping northwards, has been tilted and overturned due to north-directed folding, as illustrated in Fig. 3. The occurrence of Albian-Cenomanian clastics beneath the unfolded (northward-dipping) part of the thrust (Bacassan area, Fig. 3) is consistent with this interpretation of a south-directed thrust plane (D1). The backfolded (D2) upper part of the thrust is clearly visible further east, as shown by the V-shape intersection with the topographic surface (Casteras, Paris et al., 1971).

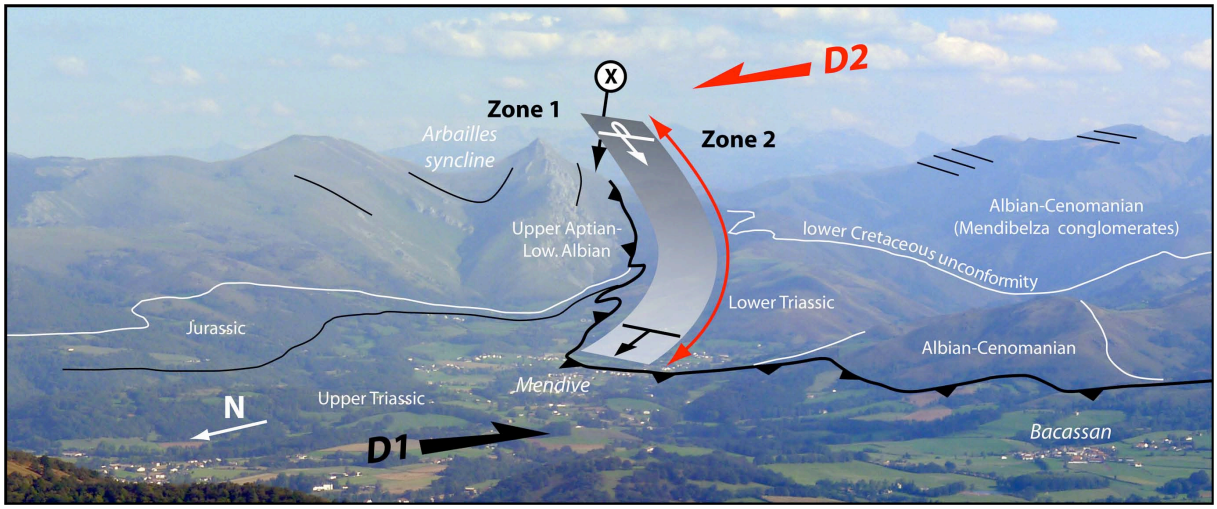

Figure 3: *~~B~~oundary between zone 1 and zone 2, west of the Arbailles massif. The Mesozoic sedimentary gap increases dramatically across this boundary, ranging from lower Jurassic to upper Cretaceous to the south of it. The thrust bounding zones 1 and 2 is folded by D2, so that its upper part shows an apparent normal, southward-dipping offset. 2 km south from the crest (locality X), both the thrust plane and the Jurassic layers of the southern limb of the Arbailles syncline are overturned and thus dipping ~60° SSW-wards, as shown by their V-shape intersections with the topographic surface (Casteras, Paris et al., 1971). Panoramic view from Pic de Jara, near St Jean-Pied de Port (looking ESE), location on fig. 2.*

Northward-verging overturned folding of the boundary thrust between zones 1 and 2 is also clearly visible to the south of Arette city (Fig. 4). The 1:2 boundary thrust is dipping southwards (Fig. 4B), which is unexpected: the Jurassic-Lower Cretaceous series which initially formed the hangingwall of the thrust are overturned together with it, so that the Igountze conglomerate unit of zone 2 (lateral equivalent of the Mendibelza conglomerates), initially located in the footwall, are presently overlying zone 1. This backfolding event (D2) probably also tilted and steepened the D1 thrusts and associated ramp anticlines of Sarrance and Mail Arrouy (more than 60° according Lagabrielle et al., 2010), together with the boundary thrust between zones 2 and 3 (Eaux Chaudes-Lakhoura thrust, ECLT) whose dip increases locally to ~30 to 40° (Ternet et al, 2004). The involvement of ECLT in D2 backfolding to the north of the Axial zone is also shown in Figures 4C and 4D.

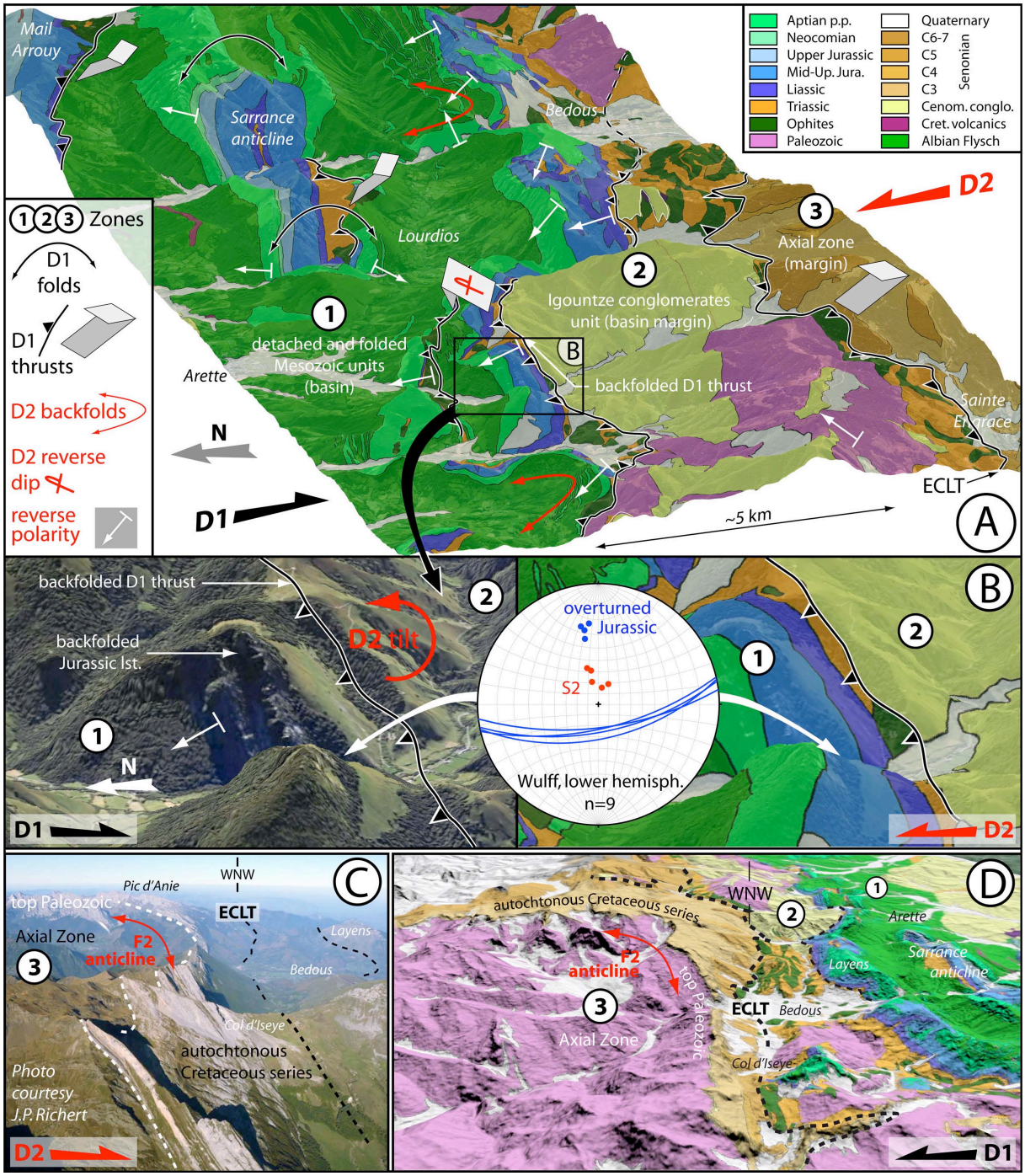

Figure 4: *Map-scale Evidence for backfolding at the southern termination of zone 1: the block diagrams and the field views give some examples of D2, north-directed structures overprinting the initial D1 tectonic buildup.*

A: Synthetic geological block diagram across zones 1 to 3, between Arette and Bedous, showing a simplified geological map draped over Aster DEM. This perspective view from WNW illustrates the D2 backfolding, with

predominantly reverse polarities involving both the Mesozoic series and the D1 boundary thrust between zones 1 and 2, and with northward-verging overturned synclines. Location of the area on Figs. 2 and 8.

B: Detailed synthetic views (landscape and geology) and structural data showing Jurassic limestones and D1 boundary thrust backfolded (and overturned) together, 5km SW of the Arette city.

C: Aerial photograph (courtesy J.P. Richert) taken from above Les Eaux Chaudes (area of fig. 5) looking westwards. This view illustrates the large-scale northward-vergent overturned fold geometry of the Axial zone (zone 3), due to D2 backfolding (red), and the resulting steepness of the ECLT and of the overlying units (zones 2 and 1) which were previously thrust over it (D1, black).

D: Westward looking block diagram corresponding to the aerial photograph of Fig. 4C (enlarged). The Axial zone shows large-scale D2 northward-vergent asymmetric folding, with a steep northern limb. The ECLT is clearly involved in this D2 folding.

4. D2/D1 overprint : structural evidence from a key area at the northern edge of the Axial Zone :

A two-phase shortening history can be documented in the key area of Les Eaux Chaudes, illustrated by the landscape views of fig. 5. The synthetic panorama of fig. 5A depicts, within the Axial Zone (zone 3), a similar relative deformation chronology as shown above within zones 1 and 2. The stratigraphic series here include a huge erosional and non-depositional gap with the Upper Cretaceous limestones unconformably lying over Paleozoic rocks (Fig. 5A; Ternet, 1965; Ternet et al., 2004). These autochtonous layers are overlain by the Eaux Chaudes thrust sheet and by Paleozoic units in the hangingwall of the ECLT. This D1, southward transported stack (black, Fig. 5A) is overprinted by D2 northward-vergent overturned folding (red, Fig. 5A). In order to document this overprint, a structural field study was carried out in this specific area which provides good outcrops and a variable relief (Fig. 5B to 5D). The tectonic units are arranged as follows, from bottom to top (Fig. 6) :

- a thin Late Cretaceous autochtonous series of Cenomanian to Santonian age (Ternet, 1965 ; Alhamawi, 1992), unconformably lying on the Eaux Chaudes granite and surrounding Devonian sediments.
- the Eaux Chaudes thrust sheet made of Cenomanian to Campanian cover locally associated with Triassic (Keuper dolomites and marls, volcanics).
- the Gourzy and Bouchouse klippes, made of Devonian schists and clastics.

The kinematic indicators associated with the emplacement of the Eaux Chaudes thrust-sheet and the Devonian klippes above are all south-directed. They are characterised by overturned folds at different scales, angular relationships between schistosity and stratification, stretching lineation and boudinage (Fig. 7). However, as shown by the interpretative cross-section of Fig. 6, the initial low-angle thrusts may have been re-deformed by steeper out-of-sequence incipient imbricates in a late D1 shortening stage. Consistently, the paleogeographic origin of the Eaux Chaudes thrust-sheet is to be found to the north of the study area, based on stratigraphic criteria : (i) Triassic rocks and Mendibelza conglomerates, which are locally associated with the thrust-sheet and are found in zone 2, could not occur further south because of their Mesozoic erosional removal beneath the Cenomanian transgressive lag all over zone 3 ; (ii) the Santonian limestones of the thrust-sheet indicate deeper open shelf environments than the autochtonous series (Alhamawi, 1992). Thus, as stated above considering kinematic indicators, the Eaux Chaudes-Lakhoura thrust outlines the southward transport of units from zone 2 over zone 3, that is from the necking zone towards the Iberian foreland. This southward directed transport occurred from Lutetian onwards (Labaume & Séguret, 1985 ; Teixell, 1996 ; Vergés & Burbank, 1996 ; Martinez-Peña & Casas-Sainz, 2003 ; Ternet et al., 2004).

Evidence for backfolding is found in the southern part of the study area (Figures 6 & 7, sites 9 to 14), as shown by the Paleozoic rocks of the high Axial Zone which are uplifted and which spectacularly overthrust northwards both the autochtonous Cretaceous cover and the Eaux Chaudes thrust-sheet (Fig. 5). The latter is clearly involved in the Arcizette overturned syncline (Ternet, 1965), mistakenly described by Izquierdo-Llavall et al. (2012) as a south-recumbent anticline. At outcrop scale, the south-verging S1 schistosity associated with the Eaux Chaudes D1 thrust is deformed by D2 backfolding (Fig. 7). Similarly, landscape views show that the Eaux-Chaudes thrust is backfolded (Figures 5B to 5D). At a regional scale, the D2 backfold appears asymmetric with a moderately steeply southward dipping axial plane. This feature explains the local steepness of the Eaux Chaudes-Lakhoura thrust (ECLT), which was clearly acquired during D2 backfolding.

This focused field analysis demonstrates the relative chronology between the southward (D1) and northward (D2) shear deformation at the northern edge of the Iberian plate.

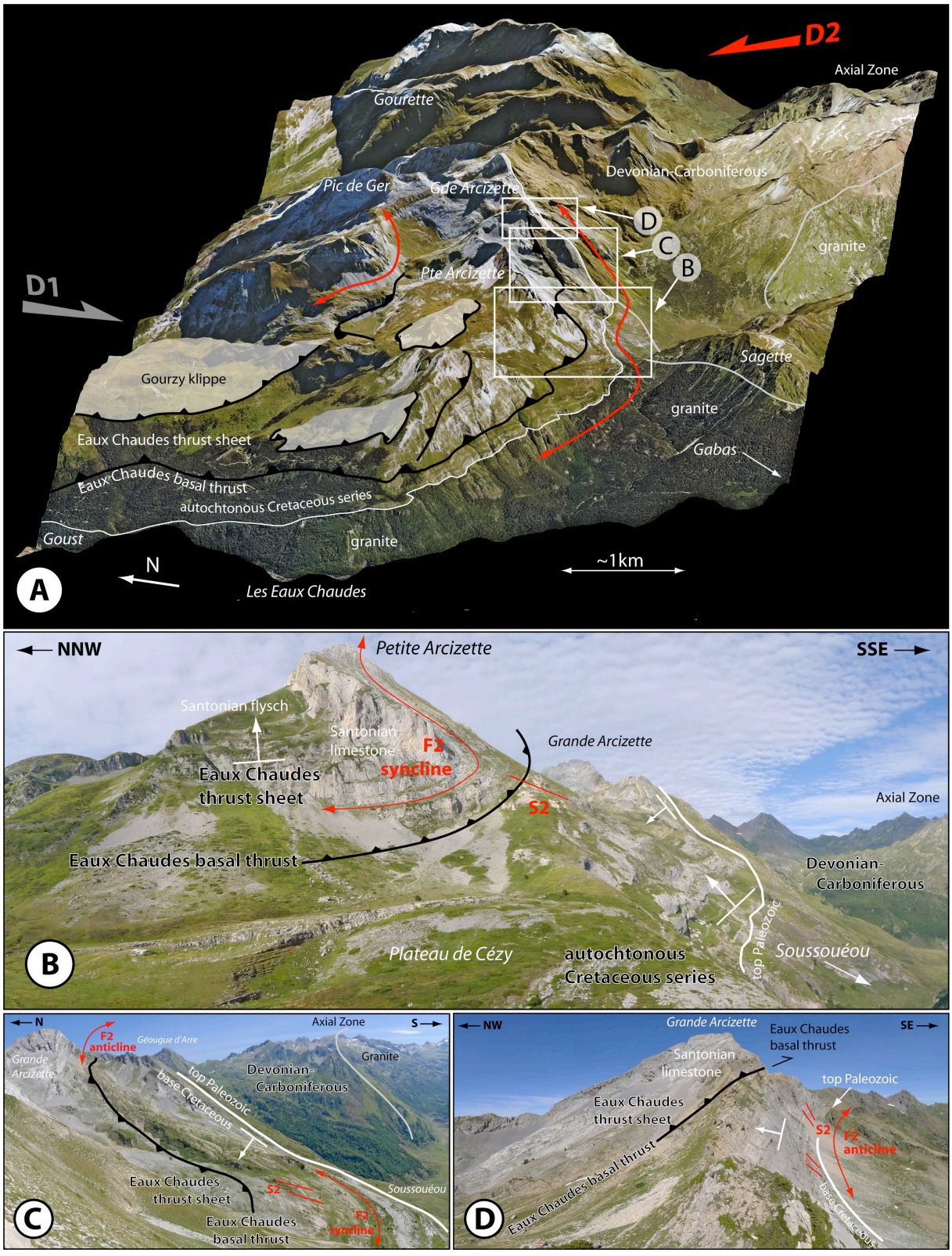

Figure 5: *A: synthetic block diagram of the Eaux Chaudes-Artouste area, built using GoogleEarth satellite view draped over Aster DEM, looking ENE. In this part of the Axial Zone (zone 3), the sedimentary gap is maximum due to rift shoulder uplift, and the upper Cretaceous (Cenomanian to Senonian) sediments are unconformably overlying the Paleozoic rocks. The south-directed D1 imbricates (black) are folded northwards by D2 (red). Location of this view on Fig. 2 and 8. The corresponding geological map and field structural observations (§4) are given in figs. 6 and 7.*

B to D: Eastward looking field panoramic views illustrating the D2 backfolds (location in A, and schematic cross section in fig. 6). The Arcizettes northward-vergent overturned folds involve both the upper Paleozoic basement, the autochtonous series of Plateau de Cézy and the D1 Eaux Chaudes basal thrust. B: lower part of the fold: synclinal hinge of Petite Arcizette, above the Plateau de Cézy, C: reverse limb of the Arcizettes recumbent fold, D: upper part: anticlinal hinge of Grande Arcizettes.

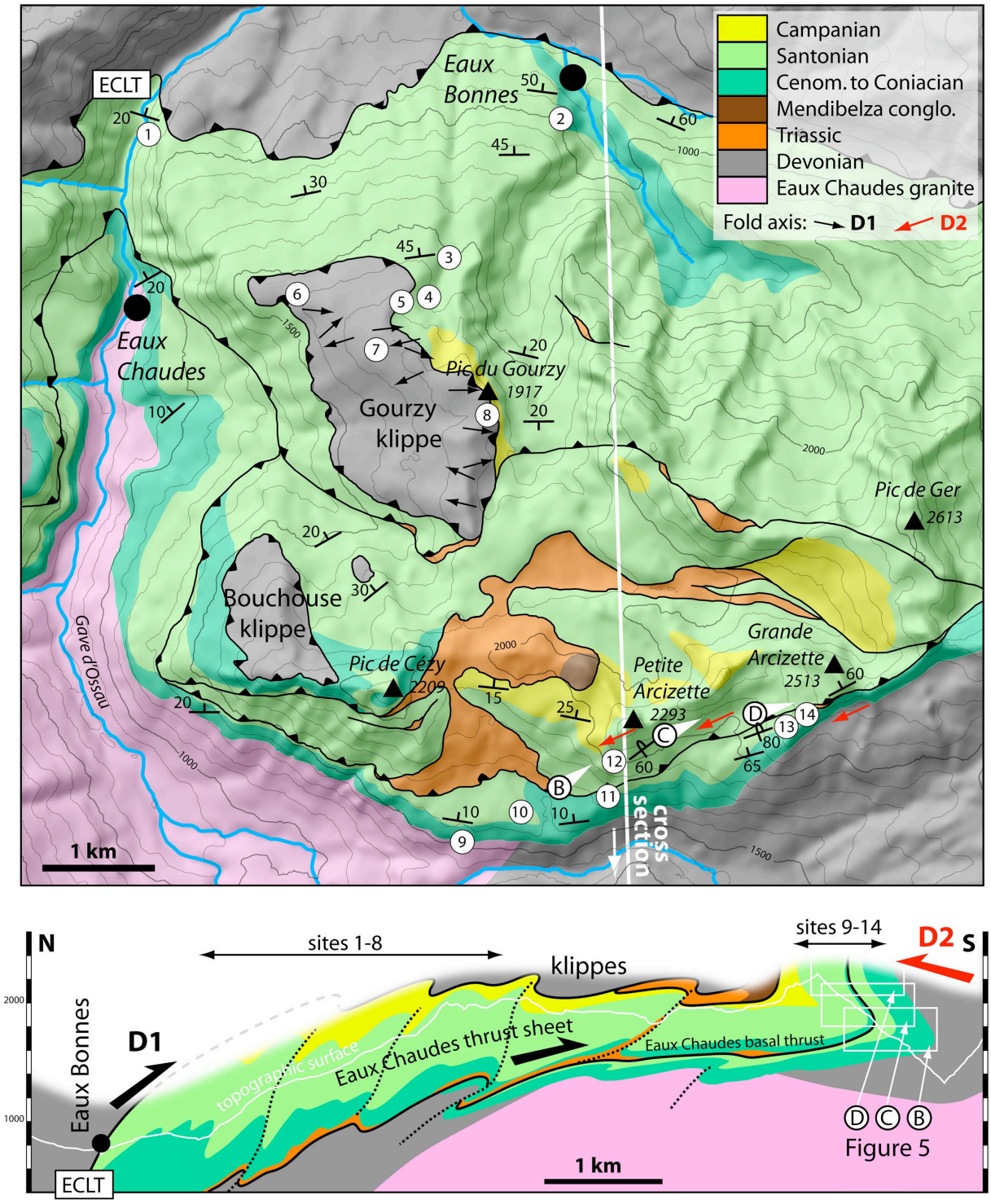

Figure 6

Geological map and interpretative cross-section of the area corresponding to fig. 5A, to the SE of Laruns (location fig. 2). Geological map modified from Ternet (1965) and Ternet et al. (2004), georeferenced. Sites 1 to 14: microstructural data presented in fig. 7 (with the addition of some D1 fold axis in the Gourzy klippe from Majesté-Menjoulas, 1979). B, C and D: location of panoramic views of Fig. 5. N-S Cross-section modified after

Ternet (1965) and personal data. The cross section demonstrates the overprint of D2 backfolding on the D1 structures. This interpretation also suggests that the D1, south-directed shear deformation is polyphase, with incipient out-of-sequence thrusting affecting the initial nappes stack. Location of the panoramic views also shown in the cross-section (projected).

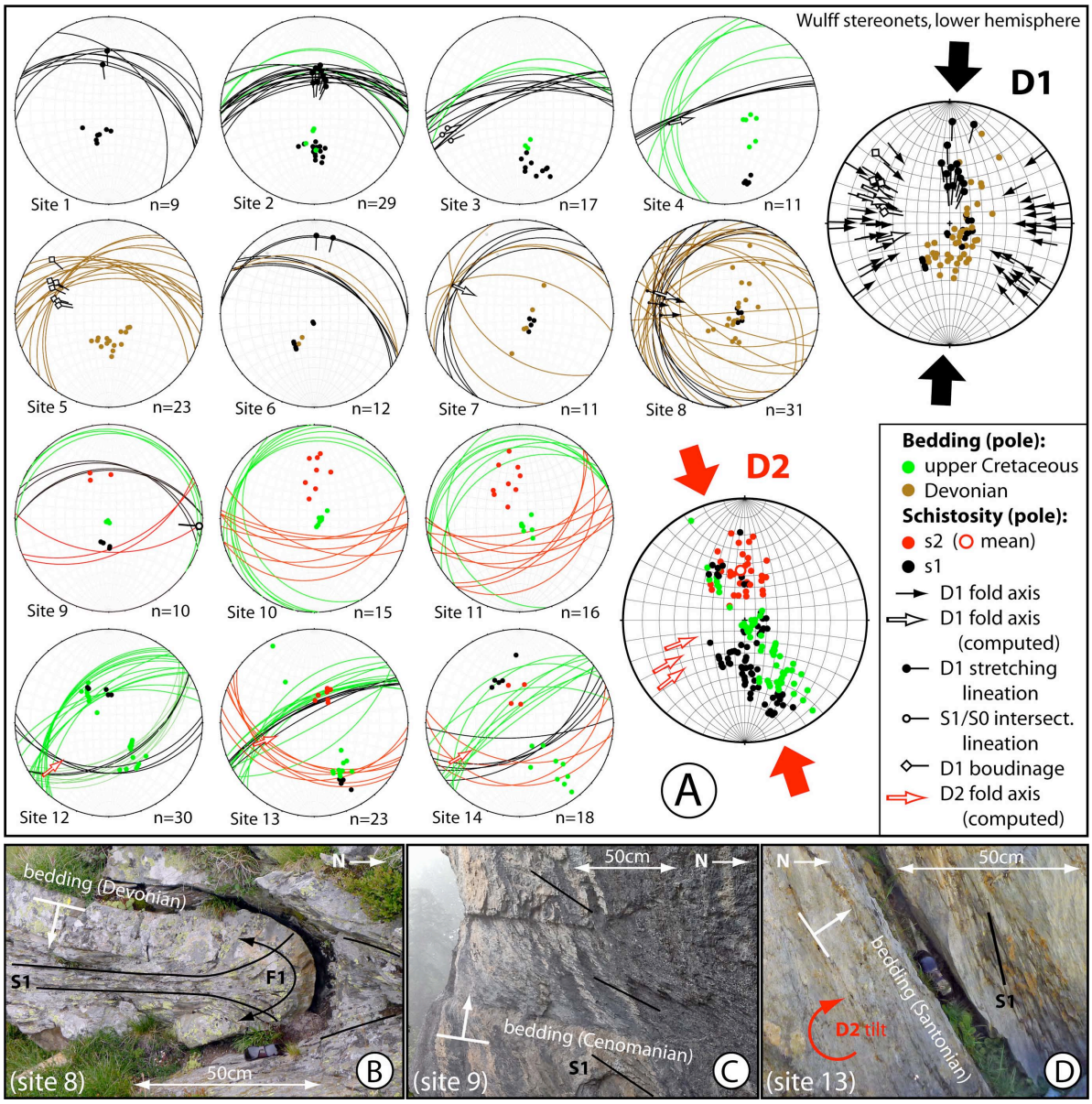

Figure 7: *A: Kinematic data in the Eaux Chaudes area, corresponding to the map of fig. 6. The northern sites (1 to 8) mainly refer to D1, south-directed shear deformation, and are located close to the ECLT main thrust. In the Devonian rocks of the Gourzy klippe, data from sites 5, 6 and 8 are located very close to the basal thrust and we consider the observed deformations, which are consistent with those in the footwall, as relevant with respect to D1 tectonic transport, and not as due to Variscan events. The data are summarized in the right, upper stereogram, with the addition of scattered D1 fold axis from Majesté (1979). The southern sites (9 to 14) reveal D2 overprint of the D1 structures: folding of Cretaceous formations together with S1 schistosity and with the Eaux Chaudes basal thrust (data summarized in the right, lower stereogram). Wulff (equal-angle) stereograms, lower hemisphere.*

B: example of D1, synschistous metric-scale south-vergent recumbent fold in the sole of the Gourzy klippe (Devonian sandstones).

C and D: low-angle obliquity between the stratification of the Cretaceous autochtonous layers and the S1 schistosity in the footwall of the D1 Eaux Chaudes basal thrust, indicating a top-to-the south shear (views looking westwards). Bedding and S1 are backfolded together (photograph D and lower, right stereogram of A), which demonstrates that D2 overprinted D1.

5. Implications for the crustal structure of the Béarn range

The interplay between the south- and north-directed compressional episodes (D1 and D2, respectively) is summarized in the block-diagram of Fig. 8. The structure of the northern part is inspired by Biteau et al. (2006) and unpublished data (J.M. Flament, pers. com. 2012). This diagram emphasizes the Eaux-Chaudes-Lakhoura thrust geometry, whose trace is undulating as a consequence of its changes in dip. We have extrapolated these dip variations at depth as shown in the cross-section. These variations of D1 thrust dip are due to D2 backfolding deformation, as exemplified in the previous field views of Figs. 3, 4 and 5. This bloc diagram also shows that the ~N110°-trending folds and thrusts of the Béarn massif (Mesozoic cover, zone 1) are oblique to the ~EW northern boundary of the uplifted basement of the high range between Bedous to the west (fig. 8) and Bagnères to the east (fig. 2). We propose that this could result from a discrepancy in direction between the D1, south- to SSW-directed transports (Velasque et al., 1989; this study) and the D2, NNW-directed backfolding (this study, section 4).

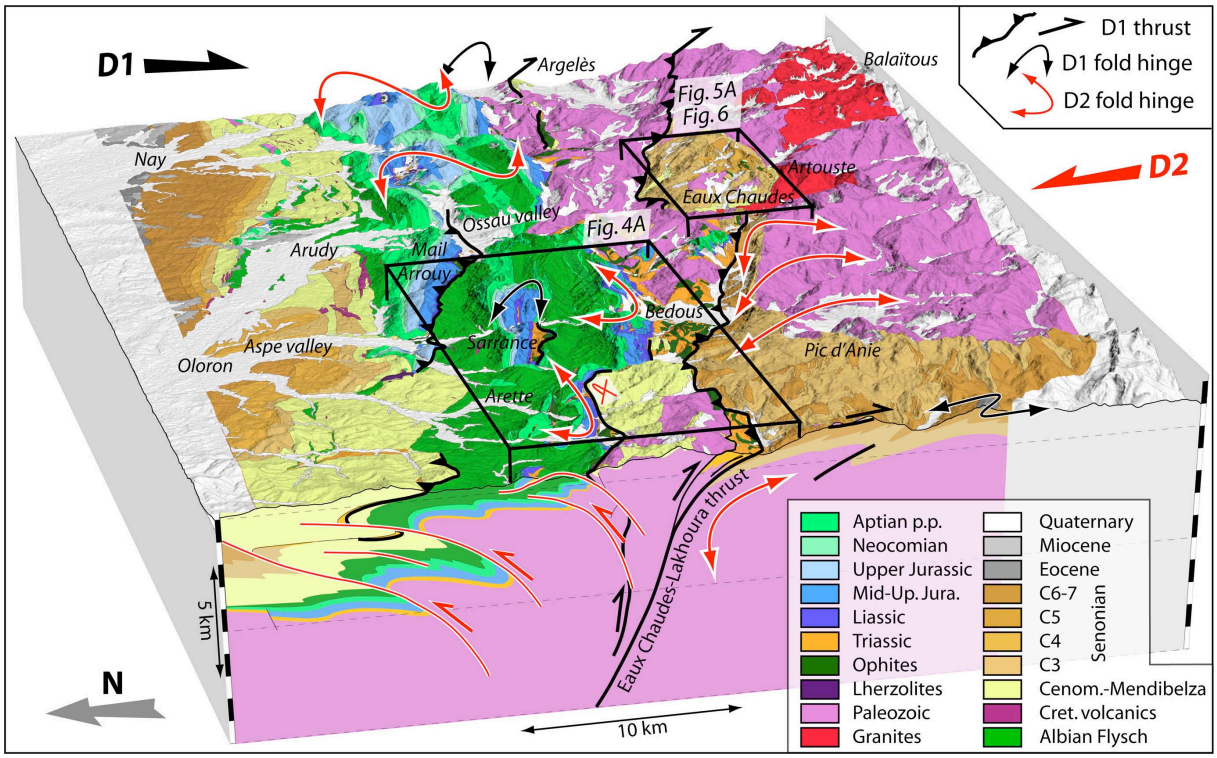

Figure 8: *Bloc diagram combining an interpretative geological cross-section located to the west of the Aspe valley (section A, fig. 1 and 10) and a simplified geological map draped on the Aster DEM. This 3D view highlights the main D1 an D2 fold-and-thrust structures (black and red, respectively) which interfer in this area. In particular, the Eaux Chaudes-Lakhoura thrust is strongly affected by D2 backfolding and is less steep at the surface than further down, as observed in the Eaux Chaudes area (fig. 4C and 4D, fig. 6). Our interpretation at depth is an extrapolation of this surface geometry..*

We interpret the present structure of the northwestern Pyrenees to result from a two-stage evolution scenario described in Fig. 9. The initial geometry (Fig. 9A) is a simplified sketch of the north-Pyrenean rift basin at the end of Early Cretaceous, which does not preclude any lithospheric thinning process having occurred before, either pure-shear or low-angle detachment. The hyperextension model which is enlightened in several recent papers (Jammes et al., 2009; Lagabrielle et al., 2010) emphasizes low-angle detachment, disruption and sliding of the pre- and syn-rift sedimentary cover. However, the study area shows a rather continuous distribution of Jurassic-Lower Cretaceous carbonate series, only folded and crosscut by thrusts and faults, which does not definitely support this model, and which is more consistent with classical crustal thinning features such as block tilting and rift-shoulder uplift. Nevertheless, during Late Cretaceous and Paleogene, this basin-margin profile was crosscut by top-to-the-south low-angle thrusts which detached the Mesozoic cover and partially involved the basement. Some of these thrusts may have reactivated extensional detachments as proposed by Velasque et al. (1989), but the very high transport distances facilitated by theses detachments as suggested by recent models (Jammes et al., 2009, Lagabrielle et al., 2010) is a matter of debate. The basement may have consisted of lower crustal or even exhumed upper mantle rocks in the central part of the rift, so that the uppermost thrust-sheets

could have sampled such kind of rocks. Some of these thrust-sheets are also marked by HT-LP metamorphism developed during crustal thinning (Montigny et al., 1986). At the end of this S-directed inversion stage (D1, Fig. 9B), the basin units (zone 1, blue) and intermediate units (zone 2, green) finally overlaid the northern edge of the normally thick Iberian crust (zone 3, orange). This stage ended during Early to Middle Eocene because the coeval sediments of the Iberian foreland are involved in this deformation (Teixell, 1996).

From Late Eocene onwards (Fig. 9C), the nappes stack is affected by top-to-the north shear developing backward-directed folds and thrusts (i.e. NPFT), while the forward thrust sequence propagated deeper into the Iberian plate (Gavarnie and more recent thrusts further south such as Bielsa or Montsech thrusts; Jolivet et al., 2007; Huyghe et al., 2009). On the northern side of the chain, this D2 backward collision stage could be a result of this forward accretion of basement thrust-sheets linked with this propagation (Teixell, 1996; Huyghe et al., 2009). This produced the onset of exhumation of the Axial Zone, which is consistent with thermochronological data (Jolivet et al., 2007; Rushlow et al., 2013).

We can thus demonstrate the occurrence in the study area of two oppositely-vergent deformation stages, a model which was proposed by Teixell (1998). It is noteworthy that the Western Alpine orogen experienced a similar and coeval two-stage evolution (Dumont et al., 2012) with increasing occurrence of backfolding. This model has some implications concerning the restoration of the Pyrenean chain. Most of the tectonic transport and shortening can be ascribed to the top-to-the south inversion stage (D1) compatible with the inferred northward continental subduction of the Iberian crust (Roure et al., 1989; Chevrot et al., 2014). This deformation acted over a previously thinned and heated crust to the north of the necking zone (Fig. 9A). Once the latter has been fully stacked in the orogen (D1, Fig. 9B), the deformation propagated within the Iberian plate itself, which induced crustal thickening and D2 backward deformation in the study area (D2, Fig. 9C). In our model, the major suture between the normal and thinned crust is an ancient feature (D1) which has been deformed and backfolded, namely the ECLT.

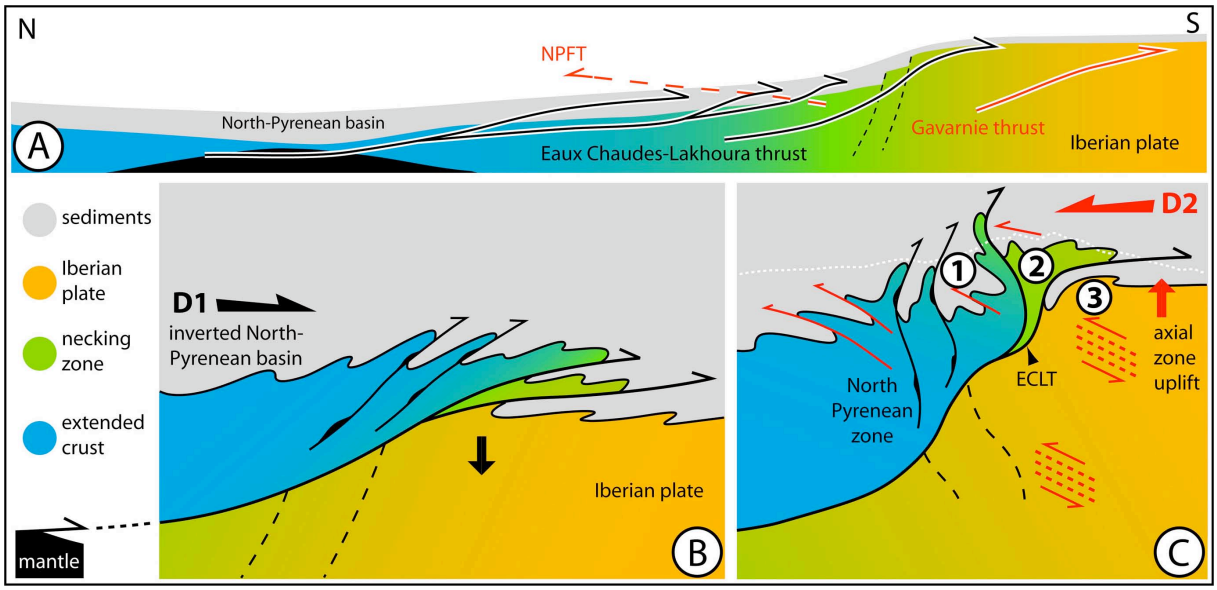

Figure 9: *Proposed multistage shortening scenario for the North-Pyrenean basin:*

A: simplified sketch at the end of Early Cretaceous, without arguing for one of the other options regarding previous processes of crustal thinning.

B: South- (or SSW-) directed inversion stage having allowed sampling of exhumed subcontinental mantle (black) and lower crust, southward transport over thicker Iberian upper crust, and shortcutting across the necking zone. This deformation stage ended during Late Eocene times, as shown by the involvement of Lower to Middle Eocene sediments further south.

C: North-directed collision stage, characterized by backfolding/backthrusting at the northern edge of the normally thick Iberian crust. This D2 deformation stage produced northward tilting and steepening of the inversion structures prepared in stage B, as shown by the present geometrical relationships between zones 1, 2 and 3 illustrated in the previous figures, but probably led to fewer tectonic transport than D1. This kinematics is consistent with uplift of the Axial Zone recorded by AFT as soon as Late Eocene-Earliest Oligocene (Jolivet et al., 2007), and possibly developped in the hangingwall of the Gavarnie thrust.

6. New clue to interpret the Béarn seismic cluster

We plotted the seismicity along three north-south cross-sections across the seismic cluster of the Béarn massif (Fig. 1; Fig. 10), in order to examine their distribution at depth with respect to the geological structure presented in this paper, deduced from both field observations and analysis of 1/50000 geological maps drapped over DEM. The depth distribution of the micro-seismicity underlines a north-dipping zone beneath the Béarn massif, down to at least 20 km (Fig. 10; Souriau and Pauchet, 1998). The core of the cluster is located beneath the Aspe valley (Oloron; Fig. 10, section B), and its shape underlines a steep (~50-60°) N-dipping zone, which tends to flatten shallowing upwards towards the south (Fig. 10; Souriau and Pauchet, 1998; Dubos-Sallée et al., 2007). This sigmoid shape is fairly consistent with the distorted trace of the ECLT at depth, as shown by Lacan (2008), Lacan & Ortuño (2012). Folding and northward steepening of the ECLT is clearly visible in our study area (Fig. 4C and 4D) and our structural data (section 4) show that it is due to D2 backfolding of an initially low-angle south-directed (D1) thrust, following the model of Fig. 9. Most of the seismic events of the Béarn cluster are located close to the interpreted prolongation at depth of the ECLT (Fig. 10), and its steepness tends to reduce the horizontal distance between the Axial Zone and the NPFT in this part of the Pyrenees (Fig. 1).

We interpret the concentrated location of the seismic events along the steep part of ECLT as follows: in this area, the steep segment of the ECLT, which was strongly affected by D2 backfolding, provides an opportunity for reactivation and favours vertical displacements at the expense of horizontal northward propagation in the foreland. By contrast, at both eastern and western extremities of the Béarn massif, a major part of compressional deformation propagated northward along south-dipping decollements, pushing the NPFT back further north. At the eastern end of the seismic cluster (Argeles; section C, Fig. 10), fewer events outline a ~50° N-dipping structure probably extending the ECLT further east. At the western extremity of the Béarn massif, a similar structure is observed below the Arbailles massif (Tardets; section A, Fig. 10A), but the seismic events may also outline moderately S-dipping structures. Very little activity is observed within the Axial Zone.

The local reactivation of the ECLT requires some vertical differential motion to the north of the Axial Zone. It has been recently shown unambiguously that the Pyrenean range is under an extensional regime at least locally, which could result from either an isostatic readjustment (uplift) of the Axial Zone possibly due to erosion (Lacan, 2008; Lacan et al., 2012; Lacan and Ortuño, 2012; Vernant et al., 2013) or a change in the regional geodynamics (Sylvander et al., 2008; Chevrot et al., 2011). Alternatively, Souriau et al. (2014) propose that the differential motion could result from subsidence of the North Pyrenean zone, driven by the occurrence at shallow depth of heavy bodies revealed by positive Bouguer anomalies. Some postorogenic normal reactivation of thrust faults reported in the highest part of the range, and located at the southern border of the seismic cluster (Lacan, 2008; Lacan and Ortuño, 2012), could have been trigger by such late extension. The observed distribution of earthquakes along steep north-dipping segments of the Eaux Chaudes-Lakhoura thrust is fairly consistent with this extensional regime. Despite the ancient character of this D1 thrust, the main triggering factor was probably D2 backtilting, which locally provided the adequate dip for extensional re-activation during the recent uplift of the Axial Zone. It is also worth noting that hydrothermal activity occurs precisely along the outcropping part of the steep ECLT segment (Eaux Bonnes and Eaux Chaudes, located on fig. 5, are famous for thermal resorts).

Our observations and interpretation shed new light on the role and significance of the so-called "North-Pyrenean fault", a confusing name in the Bearn region, that we deliberately avoid in our figures. It has been commonly regarded as a testimony of the transcurrent northern boundary of the Iberian plate (Choukroune, 1976; Choukroune & Mattauer, 1978; Séguret and Daignières, 1986; Roure et al., 1989) despite the lack of accurate field-based identification of strike-slip motion (see discussion in Souquet et al., 1977) and the fact that this boundary is by far more complex than a single fault to the west of Bagnères-de-Bigorre. In the Béarn massif, the "North-Pyrenean Fault" corresponds to a complex stack of small imbricates (Canérot et al., 2004) and in the study area it more or less coincides with the Eaux Chaudes-Lakhoura thrust zone (ECLT, Figs. 2, 8). Our interpretation is that the local steepness was acquired in a second stage of deformation, due to backfolding of an initially low-angle structure, and coeval with the uplift of the Axial Zone. This interpretation is not consistent with the interpretation of a very ancient (Cretaceous) subvertical strike-slip fault.

Figure 10 (next page): *Block diagrams across the western Pyrenees, built using a simplified geological map (after 1/50000è BRGM sheets listed below) draped on Aster DEM (Lambert 2 extended projection) and combined with three ~NS interpretative cross-sections, located on the upper left map and in fig. 1. These sections also show the location of earthquakes, projected laterally on each from a 10 km-wide slice. Catalogue OMP-IGC (Observatoire Midi Pyrénées-Institut Geològic de Catalunya) with precisely relocated events from 1997 to 2011 (for more detail see Souriau et al., 2001; Chevrot et al., 2011).*
The central section (Oloron, B) shows the major activity, which is concentrated on a narrow and steep north-dipping zone, which corresponds to the expected location of the Eaux Chaudes-Lakhoura thrust based on surface geological arguments (see text). The same observation is provided by the eastern section (Argelès, C),

although much less activity is recorded there. The western section (Tardets, A) shows more diffuse activity, suggesting that some south-dipping faults are also involved.
The simplified geological map was build after the following 1/50000è maps from BRGM: St Jean-Pied-de-Port (Le Pochat et al., 1978), Oloron (Casteras et al., 1970a), Tardets (Casteras and Paris, 1971), Lourdes (Casteras et al., 1970b), Larrau (Casteras et al., 1970c), Laruns (Ternet et al., 2004) and Argelès-Gazost (Ternet et al., 1980).

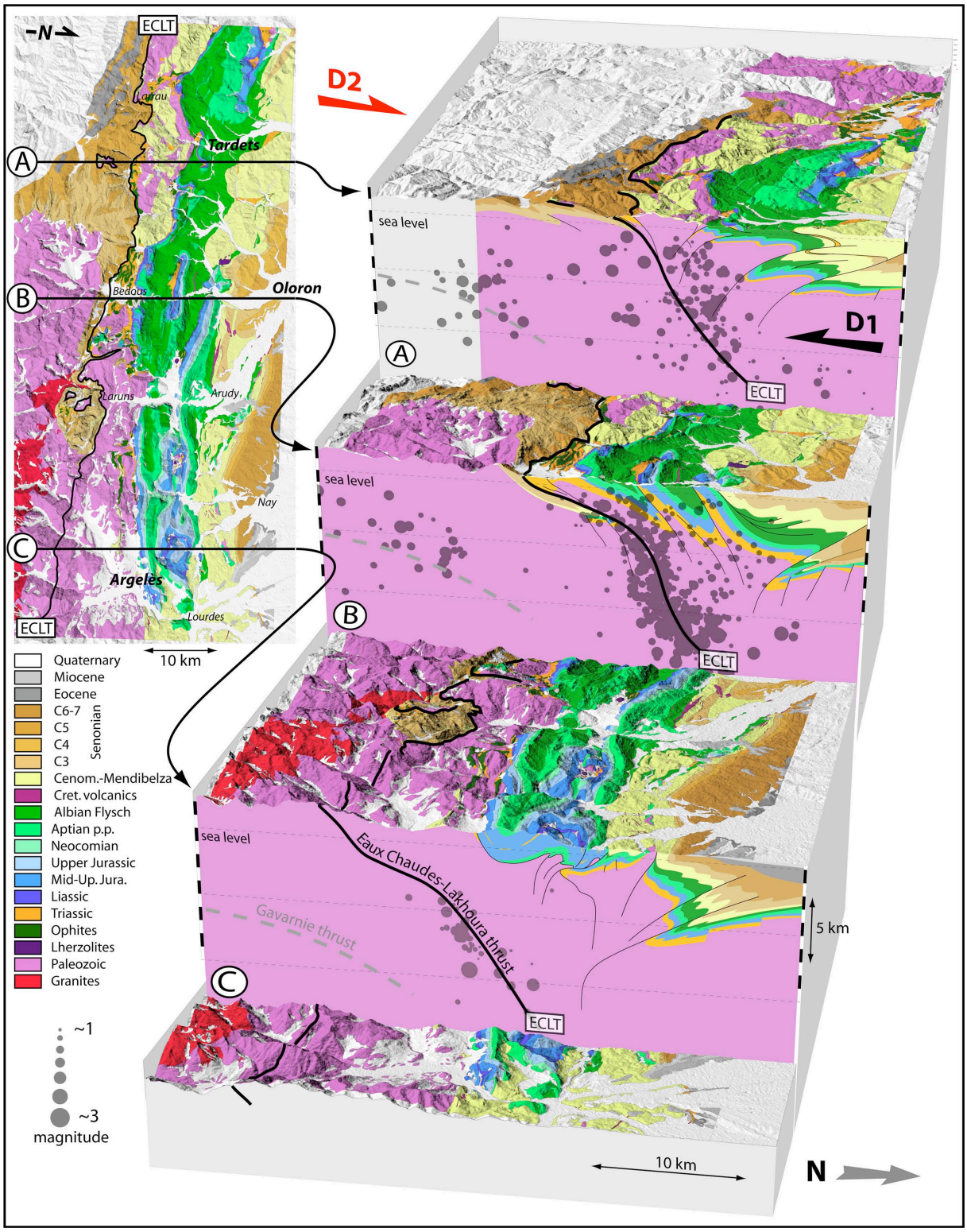

7. Conclusion

This study addresses several striking morphotectonic characters of the Béarn massif, and especially the origin of the seismic cluster located between Oloron and Bagnères-de-Bigorre (Fig. 1). This cluster occurs in a peculiar part of the Pyrenean range: firstly, the morphology of the northern part of the Béarn massif is distinctive, showing a sharp topographic step and predominantly north dipping units (Fig. 3A; Fig. 4C and 4D), whereas no topographic break is observed along the NPFT; secondly, the distance between the NPFT and the high range is the shorter along the Béarn massif than elsewhere (Fig. 1). These observations, suggest that the specific structure of the Béarn range concentrates a major part of the shortening, which limited northward propagation towards the NPFT.

Using panoramas, 3D geological information and cross-sections, we show that the structure of the Béarn massif results from the interplay between successive south- and north-directed compressional episodes. During Late Cretaceous and Paleogene, top-to-the-south low-angle thrusts detached the Mesozoic sedimentary cover of a extended crustal area (the North Pyrenean basin) and transported it southwards over the Iberian margin, with shortcuts affecting the necking zone in between (Fig. 9). From Late Eocene onwards, the early nappes stack was overprinted by backfolding, which locally tilted and steepened the previous thrusts. The steepest segment is located beneath the central part of the Béarn massif and concentrates most of the seismicity (Fig. 10). Our interpretation is that this steepest, northward dipping segment of the folded Eaux Chaudes-Lakhoura thrust locally provided the adequate dip for extensional re-activation already documented for the Pyrenean range (Sylvander et al., 2008; Lacan, 2008; Chevrot et al., 2011; Asensio et al., 2012; Lacan et al., 2012; Lacan and Ortuño, 2012; Vernant et al., 2013). At both east and west extremities of the Béarn massif, a larger part of shortening has been transferred northwards along south-dipping decollements in the foreland, as imaged by the two deep seismic profiles crossing the range (Roure et al., 1989; Grandjean, 1994; Daignières and ECORS team, 1994). Here the Eaux Chaudes-Lakhoura thrust becomes less steep, and thus less suitably orientated for extensional reactivation in response to uplift of the Axial Zone.

Aknowledgements

We gratefully aknowledge two anonymous reviewers for their constructive reviews which greatly improved the manuscript, together with Editors John Geissman and Andrei Khudoley for helpful editorial comments. We are also grateful to Steve Matthews for substantially improving the English writing. The data for this paper are available by contacting the corresponding author.

References

Aguirrezabala, L.M. and Garcia-Mondéjar J. (1992), Tectonic origin of carbonate depositional sequences in a strike-slip setting (Aptian, northern Iberia). *Sedimentary Geol., 81*, p. 163-172.

Alasset, P.J. and M. Meghraoui (2005), Active faulting in the Western Pyrenees (France): Paleoseismic evidence for the Late Holocene ruptures. *Tectonophysics, 409*, p. 39-54.

Alhamawi, M. (1992), Sédimentologie, pétrographie sédimentaire et diagenèse des calcaires du Crétacé supérieur de la marge ibérique. *PhD Thesis, University of Bordeaux,* 319 p.

Albarède, F. and Michard-Vitrac A. (1978), Age and significance of the North Pyrenean metamorphism, *Earth Plan. Sci. Lett., 40*, p. 327-332.

Asensio, E., G. Khazaradze, A. Echeverria, R.W. King and I. Vilajosana (2012), GPS studies of active deformation in the Pyrenees. *Geophys. J. Int.,* 190, p. 913-921.

Azambre, B., F. Crouzel, E.J. Debroas. J.-C. Soule and Y. Ternet (1989), Carte Géologique de la France au 1/50 000 : feuille de Bagnères-de-Bigorre, *Service Géologique National, Ed. BRGM*.

Azambre, B., J.-P. Sagon and E.-J. Debroas (1991), Le métamorphisme crétacé du fossé des Baronnies (Hautes-Pyrénées, France), témoin des anomanies thermiques de la zone transformante nord-pyrénéenne , *C. R. Acad. Sci. Paris, 313*, p. 119-124.

Baby, P., G. Crouzet, M. Specht, J. Deramond, M. Bilotte and E.J. Debroas (1988), Rôle des paléostructures albo-cénomaniennes dans la géométrie des chevauchements frontaux nord-pyrénéens, *C. R. Acad. Sc. Paris, 306*, p. 307-313.

Beaumont, C., J.A. Munõz, J. Hamilton and P. Fullsack (2000), Factors controlling the Alpine evolution of the central Pyrenees inferred from a comparison of observations and geodynamical models. *J. Geophys. Res., 105*, p. 8121-8145.

Biteau, J. J., A. Le Marrec, M. Le Vot, and J. M. Masset, (2006), The Aquitaine Basin. *Petroleum Geoscience, 12*, p. 247–273, doi:10.1144/1354-079305-674.

Boirie, J. M., and P. Souquet (1982), Les poudingues de Mendibelza: Dépôts de cônes sous-marins du rift albien des Pyrénées. *Bull. Cent. Rech. Explor. Prod. Elf Aquitaine, 6*, p. 405–435.

Bourrouilh, R., J.P. Richert and G. Zolnaï (1995), The North Pyrenean Aquitaine Basin, France: Evolution and Hydrocarbons1. *AAPG Bulletin, 79*, p. 831-853.

Canérot, J. (1989)., Rifting eocrétacé et halocinèse sur la marge ibérique des Pyrénées Occidentale (France). Conséquences structurales. *Bull. Cent. Rech. Explor. Prod. Elf Aquitaine, 13*, p. 87 – 99.

Canérot, J, Majesté-Menjoulas, C. and Ternet, Y (2004), Nouvelle interpretation structural de la "faille nord-pyrénéenne" en vallée d'Aspe (Pyrénées atlantiques). Remise en question d'un plutonisme ophitique danien dans le secteur de Bedous. *Comptes Rendus Géosciences*, 336, p. 135-142.

Canérot, J., B. Peybernès and R. Ciszak (1978), Présence d'une marge méridionale à l'emplacement de la zone des Chaînons béarnais (Pyrénées basco-béarnaises), *Bull. Soc. Géol. France, 20*, p. 673-676.

Casteras, M., J. Canerot, J.P. Paris, D. Tisin and B. Azambre (1970a), Carte Géologique de la France au 1/50 000 : feuille Oloron Sainte-Marie. *Bureau de recherches géologiques et minières,* Orléans, France.

Casteras, M., J.P. Paris et al. (1971), Carte Géologique de la France au 1/50 000 : feuille Tardets (1050), *Bureau de recherches géologiques et minières,* Orléans, France.

Casteras, M., P. Souquet, G. Culot and J. Galharague (1970c), Carte géologique de la France au 1/50 000 : feuille Larrau (1068), *Bureau de recherches géologiques et minières,* Orléans, France.

Casteras, M., A.M. Villanov, J. Godechot, J. Labourguigne and B. Azambre (1970b), Carte Géologique de la France au 1/50 000 : feuille Lourdes. *Bureau de recherches géologiques et minières,* Orléans, France.

Chevalier, M.-L., F.J. Ryerson, P. Tapponnier, R.C. Finkel, J. Van Der Woerd, Li Haibing and Liu Qing (2005), Slip-Rate Measurements on the Karakorum Fault May Imply Secular Variations in Fault Motion. *Science, 307*, doi:10.1126/science.1105466

Chevrot, S., M. Sylvander and B. Delouis (2011), A preliminary catalogue of moment tensors for pyrenean earthquakes. *Tectonophysics*, doi:10.1016/j.tecto.2011.07.011

Chevrot, S, A. Villaseñor, M. Sylvander, S. Benahmed, E. Beucler, G. Cougoulat, P. Delmas, M. de Saint Balnquat, J. Diaz, J. Gallard, F. Griamud, Y. Lagabrielle, G. Manatschal, A. Mocket, H. Pauchet, A. Paul, C. Péquegnat, O. Quillard, S. Roussel, M. Ruiz and D. Wolyniec (2014), High-resolution imaging of the Pyrenees and Massif Central from the data of the PYROPE and IBERARRAY portable array deployments. Jour. Geophys. Res., DOI :10.1002/2014JB010953

Choukroune, P. (1976), Structure et évolution tectonique de la zone nord-pyrénéenne. *Mem. Soc. Geol. France, 127*, p. 1-116.

Choukroune, P. (1992), Tectonic evolution of the Pyrenees. *Ann. Rev. Earth Plan. Sci Letters, 20*, p. 143-158.

Choukroune, P. and M. Mattauer (1978), Tectonique des plaques et Pyrenees: sur le fonctionnement de la faille transformante nord-pyrénéenne; comparaison avec les modèles actuels. *Bul. Soc. Geol. France, 7*, p. 689-700.

Combes, P.J., B. Peybernès and A.F. Leyreloup (1998), Altérites et bauxites, témoins des marges européenne et ibérique des Pyrénes occidentales au Jurassique supérieur - Crétacé inférieur, à l'ouest de la vallee d'Ossau (Pyrénées-Atlantiques, France). *C. R. Acad. Sc. Paris, 327*, p. 271-278.

Daignières, M. and ECORS team (1994), The Arzacq Eastern Pyrenees ECORS deep seismic profile. *Hydrocarbon and Petroleum Geology of France*, Eds Mascle A., Springer, 4, p. 199-208.

Debroas, E.J. (1990), Le flysch noir albo-cénomanien témoin de la structuration albienne à sénonienne de la zone nord-Pyrénéenne en Bigorre (Hautes-Pyrénées, France). *Bull. Soc. Géol. Fr., 8*, p. 273–286.

Debroas, E.J., J. Canérot and M. Bilotte (2010), Les Brèches d'Urdach, témoins de l'exhumation du manteau pyrénéen dans un escarpement de faille vraconnien-cénomanien inférieur (zone nord-pyrénéenne, Pyrénées-Atlantiques, France). *Géologie de la France, 2*, p. 53-64.

Delouis, B., H. Haessler, A. Cisternas and L. Rivera (1993), Stress tensor determination in France and neighbouring regions. *Tectonophysics, 221*, p. 413-437.

Dubos, N. (2003), Contribution à l'évaluation du risque sismique dans les Pyrenees centrales. *PhD report,* Université Toulouse III - Paul Sabatier, pp 216.

Dubos-Sallée, N, B. Niviere, P. Lacan and Y. Hervouët (2007), A structural model for the seismicity of the Arudy (1980) epicentral area (Western Pyrenees, France). *Geophys. J. Int.*, 171, p. 259-270.

Ducasse, L., P.C. Vélasque and J. Muller (1986a), Glissement de couverture et panneaux basculés dans la région des Arbailles (Pyrénées occidentales) : Un modèle évolutif crétacé de la marge nord-ibérique à l'Est de la transformante de Pamplona. *C. R. Acad. Sc. Paris, 303*, p. 1477-1482.

Ducasse, L., J. Muller and P.C. Vélasque (1986b), La chaîne pyrénéo-cantabrique: subduction hercynienne, rotation crétacée de l'Ibérie et subductions alpines différentielles. *C. R. Acad. Sc. Paris, 303*, p. 419-424.

Dumont, T., S. Schwartz, S. Guillot, T. Simon-Labric, P. Tricart and S. Jourdan (2012), Structural and sedimentary record of the Oligocene revolution in the Western Alpine arc. *Jour. Geodynamics,* 56-57, p. 18-38.

Ferrer, O., E. Roca, B. Benjumea, J.A. Muñoz and N. Ellouz (2008), The deep seismic reflection MARCONI-3 profile: Role of extensional Mesozoic structure during the Pyrenean contractional deformation at the eastern part of the Bay of Biscay. *Mar. Petr. Geol., 25*, p. 714-730.

Fortané, A., G. Duee, Y. Lagabrielle and A. Coutelle (1986), Lherzolites and the Western "Chaînons Béarnais" (French Pyrenees): structural and paleogeographical pattern. *Tectonophysics, 129*, p. 81-98.

Gagnepain, J., T. Modiano, A. Cisternas, J. C. Ruegg, M. Vadel, D. Hatzfeld, and J. Mezcua (1980), Sismicité de la région d'Arette (Pyrenees-Atlantiques) et mécanismes au foyer. *Annales Geophysicae, 36*, p. 499-508.

Gagnepain-Beyneix, J., H. Haessler, and T. Modiano (1982), The pyrenean earthquake of February 29, 1980: an example of complex faulting. *Tectonophysics, 85*, p. 273-290.

Goldberg, J.M. and A.F. Leyreloup (1990), High temperature-low pressure Cretaceous metamorphism related to crustal thinning (Eastern North Pyrenean Zone, France). *Contrib. Min. Petr., 104*, p. 194-207.

Grandjean, G. (1994), Etude des structures crustales dans une portion de chaîne et de leur relation avec les bassins sédimentaires. Application aux Pyrenees occidentales. *Bull. Centre Rech. Expl.-Prod. Elf-Aquitaine Prod., 18*, p. 391-419.

Henry, P., B. Azambre and R. Montigny (1998), Late mantle evolution of the Pyrenean sub-continental lithospheric mantle in the light of new ^{40}Ar–^{39}Ar and Sm–Nd ages on pyroxenites and peridotites (Pyrenees, France). *Tectonophysics, 296*, p. 103-123.

Huyghe, D., F. Mouthereau, S. Castelltort, P.Y. Filleaudeau and L. Emmanuel (2009), Paleogene propagation of the southern Pyrenean thrust wedge revealed by finite strain analysis in frontal thrust sheets: implications for mountain building. *Earth Plan. Sci Letters, 288*, p. 421-433.

Izquierdo-Llavall, E., T. Roman-Berdiel, A. M. Casas, B. Oliva-Urcia, I. Gil-Peña, R. Soto and A. Jabaloy (2012), Magnetic and structural study of the Eaux-Chaudes intrusion : understanding the Variscan deformation in the Western Axial Zone (Pyrenees). *Int. J. Earth Sciences (Geol. Rundsch.),* 101, p. 1817-1834.

James, V., J. Canérot and J.J. Biteau (1996), Données nouvelles sur la phase de rifting atlantique des Pyrénées occidentales au Kimméridgien: la masse glissée d'Ouzous (Hautes Pyrénées). *Géologie de la France, 3*, p. 60-66.

Jammes, S., G. Manatschal, L. Lavier and E. Masini (2009), Tectono-sedimentary evolution related to extreme crustal thinning ahead of a propagating ocean: The example of the western Pyrenees. *Tectonics, 28*, doi:10.1029/2008TC002406.

Johnson, J.A. and C.A. Hall (1989), Tectono-stratigraphic model for the Massif d'Igountze-Mendibelza, western Pyrenees. *Jour. Geol. Soc. London*, 146, p. 925-932.

Jolivet, M., P. Labaume, P. Monié, M. Brunel, N. Arnaud and M. Campani (2007), Thermochronology constraints for the propagation sequence of the south Pyrenean basement thrust system (France-Spain). *Tectonics, 26*, doi :10.1029/2006TC002080

Labaume, P. and Seguret, M. (1985), Evolution of a turbiditic foreland basin and analogy with an accretionary prism : example of the Eocene South-Pyrenean basin. *Tectonics*, 4, 7, p. 661-685.

Lacan, P. (2008), Activité sismotectonique plio-quaternaire de l'ouest des pyrénées, *phD report*, Université de Pau et des Pays de l'Adour.

Lacan, P., B. Nivière, D. Rousset, and P. Sénéchal (2012), Late Pleistocene folding above the Mail Arrouy thrust, North-Western Pyrenees (France). Tectonophysics, 541-543, p. 57-68.

Lacan, P. and M. Ortuño (2012), Active tectonics of the Pyrenees : A review. *Jour. Iberian Geology, 38*, p. 9-30.

Lacombe, O. and F. Mouthereau (1999), Qu'est-ce que le front des orogènes? L'exemple de l'orogène pyrénéen. *C. R. Acad. Sc. Paris, 329*, p. 889-896.

Lacroix, B., D. Charpentier, M. Buatier, T. Vennemann, P. Labaume, T. Adatte, A. Travé and M. Dubois (2012), Formation of chlorite during thrust fault reactivation. Record of fluid origin and P–T conditions in the Monte Perdido thrust fault (southern Pyrenees). *Contr. Min. Petrogr., 163*, p. 1083-1102.

Lagabrielle, Y., P. Labaume and M. de Saint Blanquat (2010), Mantle exhumation, crustal denudation, and gravity tectonics during Cretaceous rifting in the Pyrenean realm (SW Europe): Insights from the geological setting of the lherzolite bodies. *Tectonics, 29*, doi: 10.1029/2009TC002588

Lasserre, C., P.H. Morel, Y. Gaudemer, P. Tapponnier, F.J. Ryerson, G.C.P.King, F. Metivier, M. Kasser, M. Kashgarian, L. Baichi, L. Taiya and Y. Daoyang (1999), Postglacial left slip rate and past occurrence of M 8 earthquakes on the western Haiyuan fault, Gansu, China. *J. Geophys. Res.,* 104, p. 17633-17651.

Lenoble, J.L., and J. Canérot (1993), Sequence stratigraphy of the Clansayesian (Uppermost Aptian) formations in the western Pyrenees (France). *Spec. Publ. Int. Ass. Sediment., 18*, p. 283-294.

Le Pochat, G., M. Lenguin, J.C. Napias, C. Thibaut P. Roger and J.P.Bois (1978), Carte géologique de la France au 1/50 000 : feuille St Jean-Pied-de-Port (1049), *Bureau de recherches géologiques et minières,* Orléans, France.

Majesté-Menjoulas, C. (1979). Evolution alpine d'un segment de la chaîne varisque. Nappe de Gavarnie, chevauchements Cinq-Monts-Gentiane (Pyrénées centrales et occidentales). Thesis University of Toulouse, 343p.

Martinez-Peña, M. and A. Casas-Saintz (2003), Cretaceous-Tertiary inversion of the Cotiella Basin (southern Pyrenees, Spain). *Int. Jour. Earth Sci.,* 92, p. 99-113.

Masini, E. (2011), l'évolution tectono-sédimentaire syn-rift des bassins de marge passive profonde : exemples du bassin de Samedan (Alpes centrales, Suisse) et du bassin de Mauléon (Pyrénées basques françaises). *PhD report*, University of Strasbourg, 210p,

Montigny, R., B. Azambre, B. Rossy and R. Thuizat (1986), K-Ar study of Cretaceous magmatism and metamorphism in the Pyrenees: age and length of rotation of the Iberian peninsula. *Tectonophysics, 129*, p. 257-273.

Muñoz, J. A., (1992), Evolution of a continental collision belt: ECORS-Pyrenees crustal balanced cross-section. *Thrust Tectonics,* Ed. K. R. McClay, Chapman & Hall, p. 235-246.

Muñoz, J. A. (2002), Alpine tectonics I: the Alpine system north of the Beltic Cordillera: The Pyrenees. *The Geology of Spain*, Eds. W. Gibbons y T. Moreno, Geological Society, London, p. 370-385.

Nicolas, M., J.P. Santoire and P.Y. Delpech (1990), Intraplate seismicity: new seismotectonic data in Western Europe. *Tectonophysics, 179*, p. 27-53.

Nocquet, J. M., and E. Calais (2003), The crustal velocity field in Western Europe from permanent GPS array solutions, 1996-2001. *Geophys. J. Int., 154*, p. 72-88.

Oliva-Urcia, B., T. Roman-Berdiel, A.M. Casas, E.L. Pueyo and C. Osacar (2010), Tertiary compressional overprint on Aptian-Albian extensional magnetic fabrics, North-Pyrenean Zone. *Jour. Struct. Geol., 32*, p. 362-376.

Olivet, J. L. (1996), La cinématique de la plaque Ibérique. *Bull. Cent. Rech. Explor. Prod. Elf Aquitaine, 20*, p. 131 – 195.

Pedreira, D., Pulgar J.A., Gallart J. and Torné M. (2007), Three-dimensional gravity and magnetic modeling of crustal indentation and wedging in the western Pyrenees-Cantabrian Mountains. *J. Geophys. Res., 112*, doi:10.1029/2007JB005021

Peybernès, B. and P. Souquet (1984). Basement blocks and tectono-sedimentary evolution in the Pyrenees during Mesozoic times. Geological Magazine, 121, 397-405.

Puigdefabregas, C. and P. Souquet (1986), Tecto-sedimentary cycles and depositional sequences of the Mesozoic and Tertiary from the Pyrenees. Tectonophysics, 129, p. 173-203.

Replumaz, A., R. Lacassin, P. Tapponnier and P.H. Leloup (2001), Large river offsets and Plio-Quaternary dextral slip rate on the Red River fault (Yunnan, China). *J. Geophys. Res.,* 106, p. 819-836.

Rigo, A., A. Souriau, N. Dubos, M. Sylvander and C. Ponsolles (2005), Analysis of the seismicity in the central part of the Pyrenees (France), and tectonic implications. *Journal Seismology, 9*, p. 211–222.

Rigo, A., P. Vernant, K.L. Feigl, X. Goula, G. Khazaradze, J. Talaya, L. Morel, J. Nicolas, S. Blaize, J. Chéry and M. Sylvander (2014), Present-day deformation of the Pyrenees revealed by GPS surveying and earthquake focal mechanisms until 2011. *Geophys. Jour. Int.,* in revision.

Roure, F., P. Choukroune, X. Berastegui, J. A. Muñoz, A. Villien, P. Matheron, M. Bareyt, M. Seguret, P. Camara, and J. Deramond (1989), ECORS deep seismic data and balanced cross sections: Geometric constraints to trace the evolution of the Pyrenees. *Tectonics, 8*, p. 41-50.

Rushlow, C.R., J.B. Barnes, T.A. Ehlers and J. Vergés (2013), Exhumation of the Southern Pyrenean fold-thrust belt (Spain) from orogenic growth to decay, *Tectonics, 32,* p. 1-18, doi: 10.1002/tect.20030.

Seguret, M., and M. Daignieres (1986), Crustal-scale balanced cross-sections of the Pyrenees; discussion. *Tectonophysics, 129*, p. 303-318.

Sibuet, J. C., S. P. Srivastava and W. Spackman (2004), Pyrenean orogeny and plate kinematics. *J. Geophys. Res., 109*, doi:10.1029/2003JB002514

Soto, R., M. Casas-Sainz and J.J. Villalain (2011), Widespread Cretaceous inversion event in northern Spain: evidence from subsurface and palaeomagnetic data. *Jour. Geol. Soc. London, 168*, p. 899-912.

Soula, J.C., C. Lamouroux, P. Viallard, G. Bessiere, P. Debat and B. Ferret (1986), The mylonite zones in the Pyrenees and their place in the Alpine tectonic evolution. *Tectonophysics, 129*, p. 112-147.

Souquet, P., E.J. Debroas, J.M. Boirie, P. Pons, G. Fixari, J.C. Roux, J. Dol, J.P. Thieuloy, M. Bonnemaison, H. Minvit and B. Peybernès (1985), Le groupe du Flysch Noir (Albien-Cénomanien) dans les Pyrénées. *Bull. Centres Rech. Exp. Prod. Elf Aquitaine, 9*, p. 183-252.

Souquet, P., B. Peybernès, M. Bilotte and E.J. Debroas (1977), La chaine alpine des Pyrénées. *Géologie Alpine,* 53, p. 193-216.

Souriau, A. and H. Pauchet (1998), A new synthesis of Pyrenean seismicity and its tectonic implications. *Tectonophysics, 290*, p. 221-244.

Souriau, A., A. Rigo, M. Sylvander, S. Benahmed and F. Grimaud (2014), Seismicity in central-western Pyrenees (France) : A consequence of the subsidence of dense exhumed bodies. *Tectonophysics*, 621, p. 123-131.

Souriau, A., M. Sylvander, A. Rigo, J.F. Fels, J.M. Douchain and C. Ponsolles (2001), Sismotectonique des Pyrenees: principales contraintes sismologiques. *Bull. Soc. Géol. Fr., 172*, p. 25-39.

Sylvander, M., A. Souriau, A. Rigo, A. Tocheport, J.P. Toutain, C. Ponsolles and S. Benhamed (2008), The 2006 November, ML=5.0 earthquake near Lourdes (France): new evidence for NS extension across the Pyrenees. *Geophys. J. Int., 175*, 649-664, doi: 10.1111/j.1365-246X.2008.03911.x.

Teixell, A. (1996), The Anso transect of the southern Pyrenees: Basement and cover thrust geometries. *Jour. Geol. Soc. London, 153*, p. 301-310.

Teixell, A. (1998), Crustal structure and orogenic material budget in the west central Pyrenees. *Tectonics, 17*, p. 395-406.

Ternet, Y. (1965), Etude du synclinal complexe des Eaux-Chaudes (Basses-Pyrénées). *PhD Thesis, University of Toulouse,* 152 p.

Ternet, Y., P. Barrère and J.P. Bois (1980), Carte géologique de la France au 1/50 000 : feuille Argelès-Gazost (1070), *Bureau de recherches géologiques et minières,* Orléans, France.

Ternet, Y., C. Majesté-Menjoulas, J. Canérot, T. Baudin, A. Cocherie, C. Guerrot and P. Rossi (2004), Notice explicative, Carte géologique de France (1/50000), feuille Laruns-Somport (1069), Orléans, BRGM, 192p.

Velasque, P.C., and L. Ducasse (1986), Tectonique et sédimentation dans la couverture crétacée des Pyrénées occidentales (Haute Soule). Argument en faveur de la subduction de la plaque ibérique sous la plaque européenne. *C. R. Acad. Sc. Paris, 302*, p. 1027-1032.

Velasque, P.C., L. Ducasse, J. Muller and R. Scholten (1989), The influence of inherited extensional structures on the tectonic evolution of an intracratonic chain : the example of the Western Pyrenees. *Tectonophysics, 162*, p. 243-264.

Verges, J. and D.W. Burbank (1996), Eocene-Oligocene thrusting and basin configuration in the Eastern and Central Pyrenees (Spain), *In:* Friend, P.F. and C.J. Dabrio (Eds.), Tertiary basins of Spain. The stratigraphic record of crustal kinematics, *World and regional geology, Cambridge University Press,* p. 120-133.

Verges, J., H. Millan, E. Roca, J.A. Muñoz, M. Marzo, J. Cirés, T. Den Bezemer, R. Zoetemeijer and S. Cloething (1995), Eastern Pyrenees and related foreland basins – Precollisional, syncollisional and postcollisional crustal-scale cross-sections. *Mar. Petr. Geol., 12*, p. 903-915.

Vernant, P., F. Hivert, J. Chery, P. Steer, P. Cattin and A. Rigo (2013), Erosion-induced isostatic rebound triggers extension in low convergent mountain ranges, *Geology 41(4)*: 467-470.